Civil and Sustainable Urban Engineering

Research Article
Volume 3(1), 2023, 25-39
https://doi.org/10.53623/csue.v3i1.180

Structural Behaviour of Reinforced Concrete Beam with Embedded Polystyrene Spheres

Jen Hua Ling*, Ji Wei Lau, Yong Tat Lim

Centre for Research of Innovation & Sustainable Development, School of Engineering and Technology, University of Technology Sarawak, 96000 Sibu, Sarawak, Malaysia.

*Correspondence: lingjenhua@uts.edu.my

SUBMITTED: 1 January 2023; REVISED: 2 February 2023; ACCEPTED: 5 February 2023

ABSTRACT: The beam is a structural element in a reinforced concrete structure. However, its weight places additional strain on the columns and foundations.Polystyrene spheres can be used to replace concrete in a beam to reduce its weight. However, this can affect the beam's structural performance. This study investigated the behavior of beams with embedded polystyrene spheres under loads. The purpose was to determine the feasibility of this technique. Six beam specimens, including a control specimen, were tested under the four-point load setup. The polystyrene spheres' diameter ranged from 50 mm to 75 mm. The spacing between the spheres varied from 10 mm to 30 mm. By replacing 8.7% of the concrete, the beam's strength increased by 8% per unit of concrete. The polystyrene spheres marginally altered the load capacity but reduced the stiffness, uncracked load, and ductility. The load capacity decreased by 2.6% as the polystyrene sphere's diameter increased from 50 mm to 10 mm. The strength increased by 0.6% as the spacing increased from 10 mm to 30 mm. For satisfactory performance, the polystyrene spheres with a diameter of 0.57 times the beam's width may be spaced at 1.2 times the concrete cover.

KEYWORDS: Reinforced concrete beam; polystyrene spheres; flexural behaviour; four-point load test; concrete replacement.

1. Introduction

The beam is a crucial structural element in reinforced concrete (RC) structures. It is a part of the skeletal frame system. It resists loads acting perpendicularly to the beam's axis [1]. One problem with RC members is their weight. The weight puts extra load on the columns and foundations. Thus, larger columns and foundations are required. The weight of RC beams can be reduced by partially removing the concrete. This can be done by creating voids or embedding lightweight materials in the beam (Table 1). This approach is conceptually viable based on the beam's bending theory. The concrete in the tension zone is expected to convey no load, which may reach 80% of the total concrete volume [2]. Even so, that concrete cannot be fully removed, as this can significantly affect the beam's performance. The biggest challenge in removing concrete from beams is achieving structural performance comparable to that of a solid beam. Excessive concrete removal can affect the beam's stiffness, load capacity, and ductility [20, 27, 28]. It may also reduce the shear strength of the beam and result in brittle

failure [29]. The material's efficiency can also be a concern for these beams. The beam can lose more strength than weight, in percentage [30]. Thus, this kind of beam needs to be comprehensively investigated, particularly to uncover the factors governing its structural performance.

Table 1. Previous studies of lightweight beams.

Method	Materials	Reference
Creating voids in beams	PVC pipe	[1, 3–10]
	Plastic ball or void former	[11–15]
	Plastic bottle	[16–18]
	Seeding tray	[19]
Embedded lightweight materials	Polystyrene spheres	[20]
	Polystyrene block	[21–24]
	Foamed concrete infill	[25]
	Polypropylene Plastic Sheet	[26]

There were studies on beams embedded with various lightweight materials, but only a limited number involved polystyrene spheres (Table 1). Most studies compared the beam's strength with that of the solid beams, but not many looked into the material efficiency, which is the strength per unit of concrete. This paper presents an experimental study of beams with embedded polystyrene spheres. The purpose was to investigate the behavior of the beams. The effects of the size of the polystyrene spheres and the spacing between the polystyrene spheres were examined. Then, the feasibility of having polystyrene spheres in RC beams was analyzed. Material efficiency would be one of the evaluation criteria for feasibility.

2. Materials and Methods

In this study, RC beams embedded with polystyrene spheres were tested under an incremental monotonic load. This was hypothesised that polystyrene spheres would reduce the beams' strength but increase the strength per unit weight.

2.1. Specimens.

Six beam specimens were fabricated. This included one control (i.e., CB) and five test specimens (i.e., PB1 to PB5). The control specimen was a solid beam. It represented the beam's response without the influence of the polystyrene spheres. The test specimens had polystyrene spheres embedded in the beams (Figure 1). The polystyrene spheres were placed at the centroid of the beam's cross-section. The sphere's diameter ranged from 50 mm to 100 mm, whereas the spacing between the spheres was between 10 mm and 30 mm (Table 2).

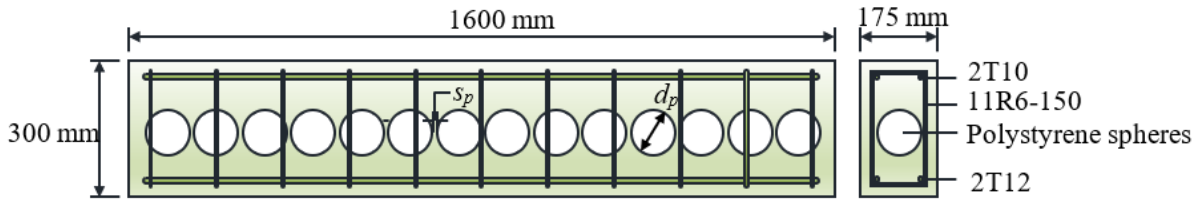

Figure 1. Schematic drawing of the test specimen.

The specimen size was 175 mm by 300 mm by 1600 mm. The concrete cover was 25 mm thick. High-strength steel bars with a nominal yield strength of 500 N/mm^2 were used as reinforcements. The top bars were 10 mm in diameter, whereas the bottom bars were 12 mm in diameter. The shear links were mild steel bars with a nominal yield strength of 250 N/mm^2. They were 150 mm apart and 6 mm in diameter.

Table 2. Details of specimens.

Specimen	Diameter of polystyrene sphere, d_p (mm)	Spacing between polystyrene spheres, s_p (mm)	Number of polystyrene spheres, np (units)
CB	-	-	-
PB1	50	10	25
PB2	75	10	18
PB3	100	10	14
PB4	100	20	12
PB5	100	30	11

The specimens were cast in timber formworks (Figure 2(a)). Before casting, steel reinforcements were prepared. The polystyrene spheres were tied to the reinforcement using galvanised wires (Figure 2(b)). The specimens were cast using C20/25 ready-mix concrete with the designed slump of 100 mm to 180 mm. For curing, the specimens were sprayed with water and covered with plastic sheets. The specimens were tested 28 days after casting.

(a) Formworks (b) Steel reinforcements and polystyrene spheres

Figure 2. Formworks of specimens.

2.2. Test setup.

The specimens were tested under the four-point load test setup (Figure 3). Each specimen sat on two rockers with a clear span of 1500 mm. A hydraulic jack was used to impose force on a distribution beam. The distribution beam then transmitted the force to the specimen through the two steel rockers. The distance between the rockers was 260 mm.

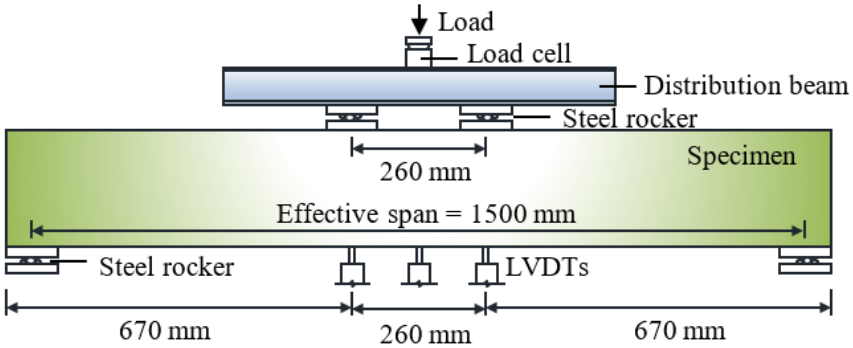

Figure 3. Test setup of the specimen.

A load cell was used to measure the load applied to the specimen. It was placed between the hydraulic jack and the distribution beam. Three Linear Variable Differential Transformers (LVDTs) were used to measure the specimen's deflection. One LVDT was installed in the mid-span, and two more were installed below the rockers. All the measuring instruments were connected to a data logger for data acquisition. The equipment and instruments used for testing are given in Table 3.

Table 3. Equipment and instruments used for testing.

Equipment	Model, Manufacturing country	Capacity	Accuracy
Hydraulic Jack	Enerpac RR-10018, North America	933 kN load	-
Hydraulic Pump	Enerpac P-462, North America	700 bar operating pressure	-
LVDT	TML CDP-100, Japan	100 mm stroke	± 0.01 mm
Load Cell	TML CLJ-300KNB, Japan	Capacity 300kN	± 0.1 kN
Data logger	TML TDS-630, Japan	50 Channels	0.1s measurement speed

2.3. Test procedure.

The test was carried out following the procedure described by the previous researchers [20, 21, 22]. The specimen was first preloaded to 10% of the estimated ultimate capacity for about 5 minutes to consolidate the test setup. The preload was then released for 1 minute for recovery. This process was repeated twice to check the test setup and the measuring devices. Then, all the readings were reinitialized to zero. The load was gradually increased at an interval of about 5 kN or 0.5 mm, whichever was achieved first. The purpose was to acquire smooth load-displacement plots. The load was held in place for at least one minute. Readings were taken once the load stabilized. Throughout the test, the specimen's surface was inspected to monitor the cracks. The test was stopped after three consecutive drops in the readings given by the load cell.

3. Results and Discussion

The test results comprised the material properties, geometrical properties, load-displacement responses, failure modes, and mechanical properties of the specimens. Then, the effects of polystyrene spheres on the beams' stiffness, strength, and ductility are discussed.

3.1. Material properties.

The properties of the materials used to fabricate the specimens are shown in Tables 4 and 5. The concrete strengths were higher than the designed cube strength of 25 N/mm^2. The reinforcements and shear links achieved their nominal strengths of 500 N/mm^2 and 250 N/mm^2 respectively. Hence, the quality of materials was considered acceptable.

Table 4. Compressive strength of concrete.

Specimen	Compressive Strength, f_{cu} (N/mm^2)[1]		Average Compressive Strength, $f_{cu,\,avg}$ (N/mm^2)
	Cube 1	Cube 2	
CB 1	27.1	26.7	26.9
PB 1	26.8	26.8	26.8
PB 2	26.6	26.2	26.4
PB 3	26.3	26.7	26.5
PB 4	26.6	26.8	26.7
PB 5	26.9	27.1	27.0

[1] Results obtained from 150 mm cube samples.

Table 5. Yield strength of steel bar.

Bar Diameter (mm)	Yield Strength, f_y (N/mm^2)			Average Yield Strength, $f_{y,avg}$ (N/mm^2)
	Sample 1	Sample 2	Sample 3	
R6	290	279	285	284.7
T10	640	635	638	637.7
T12	670	660	650	660.0

3.2. Geometrical properties.

The polystyrene spheres partially replaced the concrete in the specimen. An area replacement ratio, R_a, quantified the effective concrete area of the beam's cross-section (Eq. 1).

$$R_a = \frac{A_p}{A_b} \quad (1)$$

where A_p = Cross-sectional area of polystyrene spheres, mm^2; A_c = Cross-sectional area of the solid beam, mm^2.

The volume replacement ratio, R_v, represented the effective concrete volume of the entire beam (Eq. 2).

$$R_v = \frac{V_p}{V_b} \quad (2)$$

where V_p = total volume of polystyrene spheres, mm^3; V_c = volume of the solid beam, mm^3.

The volumes of polystyrene spheres V_p, and solid beam V_s, were computed using Eqs. 3 and 4, respectively.

$$V_p = \frac{1}{6} n_p \pi {d_p}^3 \quad (3)$$

where n_p = number of polystyrene spheres in the beam; d_p = diameter of polystyrene spheres, mm.

$$V_s = b \times h \times l \quad (4)$$

where b = width of the beam, mm; h = height of the beam, mm; l = length of the beam, mm.

The effective moment of inertia of the specimen's cross-section was computed using Eq. 5.

$$I_{eff} = I_b - I_p \quad (5)$$

where I_b = moment of inertia of solid beam, mm^4; I_p = moment of inertia of polystyrene sphere, mm^4.

The moments of inertia of a solid beam and a polystyrene sphere were calculated based on Eqs. 6 and 7.

$$I_b = \frac{bh^3}{12} \quad (6)$$

$$I_p = \frac{\pi {d_p}^4}{64} \quad (7)$$

where b = width of the beam, mm; h = height of the beam, mm; d_p = diameter of polystyrene spheres, mm.

Table 6 summarises the geometrical properties of the specimens. The results reveal that as the diameter of the polystyrene spheres rose, the area and effective moment of inertia of the beam section dropped. When the diameter of the polystyrene spheres increased and the space between the polystyrene spheres decreased, the concrete volume decreased.

Table 6. Geometrical properties.

Specimen	Cross-sectional area of polystyrene sphere, A_p (mm^2)	Area replacement ratio, R_a	Volumes of polystyrene spheres, V_p (mm^3)	Volume replacement ratio, R_v	Moment of inertia of polystyrene sphere, I_p (mm^4)	Effective moment of inertia, I_{eff} (mm^4)
Equation		**(1)**		**(2)**		**(5)**
CB1	0	0	0	0	0	393,750,000
PB1	1,963	0.037	1,636,246	0.019	306,796	393,443,204
PB2	4,418	0.084	3,976,078	0.047	1,553,156	392,196,844
PB3	7,854	0.150	7,330,383	0.087	4,908,739	388,841,261
PB4	7,854	0.150	6,283,185	0.075	4,908,739	388,841,261
PB5	7,854	0.150	5,759,587	0.069	4,908,739	388,841,261

A_b = cross-sectional area of solid beam (52500 mm^2), V_s = volumes of solid beam (84000000 mm^3), I_b = moment of inertia of solid beam (393750000 mm^4); n_p and d_p refer to Table 2; b = 175 mm, h = 300 mm, l = 1600 mm

3.3. Load-displacement responses.

The load-displacement responses of the specimens are shown in Figure 4. The specimens started with the uncracked-elastic stage. At this point, the stiffness was the highest. The concrete and reinforcements were both in good condition, allowing stress to be effectively transferred between them. The specimens entered the cracked-elastic stage after the first crack. The stiffness dropped slightly as the concrete gave way. The reinforcements then played an important role in resisting the load. The specimens gave an elastic response due to the elasticity of the reinforcements. This elastic stage ended as the reinforcement yielded. This set off the post-yield stage. For the plastic deformation of the reinforcements, significant beam deflection was observed. The failure stage happened at the ultimate state, where the load capacity peaked. The response for each stage is described in Table 7.

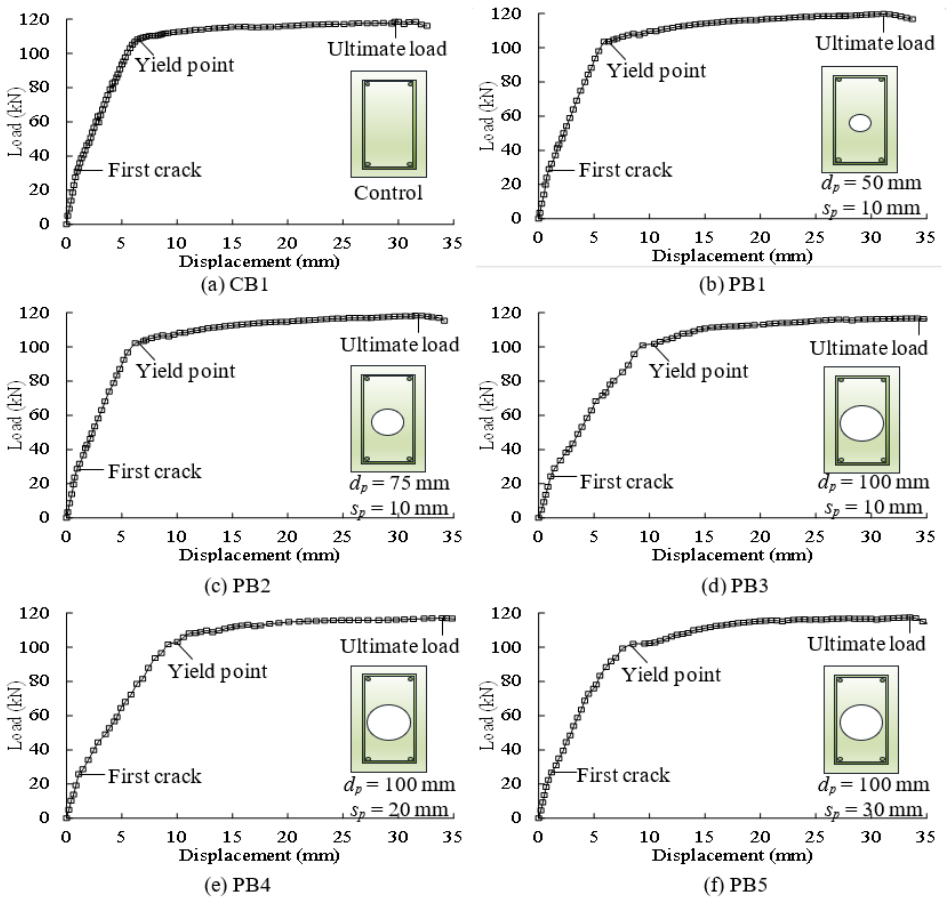

Figure 4. Test setup of specimen.

Table 7. Stages of load-displacement responses.

Stages	Description	Response
Elastic (uncracked)	The earliest stage of the specimen before the first crack.	• The entire specimen was in good condition. • The specimen's stiffness[1] at this stage was the highest. Deflection increased marginally under load. • The load-displacement curve was about linear. The deflection was nearly proportionate to the applied load.
Elastic (cracked)	The stage of the specimen after the first crack and before the yield point	• The first crack appeared in the middle of the span. As the load increased further, (a) the crack widened and propagated deeper into the beam, and (b) more cracks developed along the specimen. • The stiffness decreased slightly. The displacement increased at a faster rate. • The load-displacement curve was still close to linear. Thus, the deflection was about proportionate to the applied load.
Post-yield	The later stage of the specimen after the yield point before failure.	• The specimen's stiffness decreased drastically after the yield point. This could be due to the yielding of steel reinforcement[2] and excessive cracking of concrete. • The specimen endured plastic deformation. Considerable displacement developed with a slight increase in load.
Failure	The ultimate state of the specimen.	• The specimen experienced critical damage and thus the applied load peaked.

[1] The specimen stiffness was represented by the gradient of the load-displacement curve

[2] As strain gauge was not installed on the steel reinforcement, the yield point of the steel reinforcement was not determined.

In this study, strain gauges were not installed on the reinforcements. It was unsure whether or not the reinforcement had yielded during the test. Nevertheless, the beam specimens exhibited signs of yielding. At the post-yield stage, the beam's stiffness degraded dramatically. This was followed by a substantial deflection before reaching the ultimate state. This response was believed to be caused by the yielding process of the reinforcements.

3.4. Crack pattern and failure mode.

Cracks developed as the strain limit of the concrete was exceeded. The strain was due to the flexural stress caused by the load applied to the beam. Three types of cracks were found, namely flexural, flexural-shear, and shear cracks. These cracks are shown in Figure 5 and described in Table 8.

Table 8. Types of cracks observed.

Type	Description
Flexural crack (F)	• The first crack noticed on the beam's surface • It started from the beam soffit and slowly propagated upward as the load increased. • It was found at the mid-span of the beam, between the two point loads acting on the beam.
Flexural-shear crack (FS)	• The cracks were discovered 1.5 to 2 d away from the beam's support. • It spread vertically at first but eventually became diagonal.
Shear crack (S)	• The crack appeared within 1.5 d of the beam's support. • The crack was slanted all the way through. The angle of inclination was about 45o from the beam's soffit.

d = effective depth of the specimen

The flexural crack was first detected at around 1/4 to 1/5 of the ultimate load at the mid-span (Figure 5). As the load increased, more flexural cracks were observed. The cracked region spread sideways from the mid-span and towards the supports. Then, flexural-shear cracks appeared. Occasionally, shear cracks develop near the support. These cracks deteriorated the concrete, downgraded the bond with reinforcement, and eventually affected the load capacity of the specimens [20].

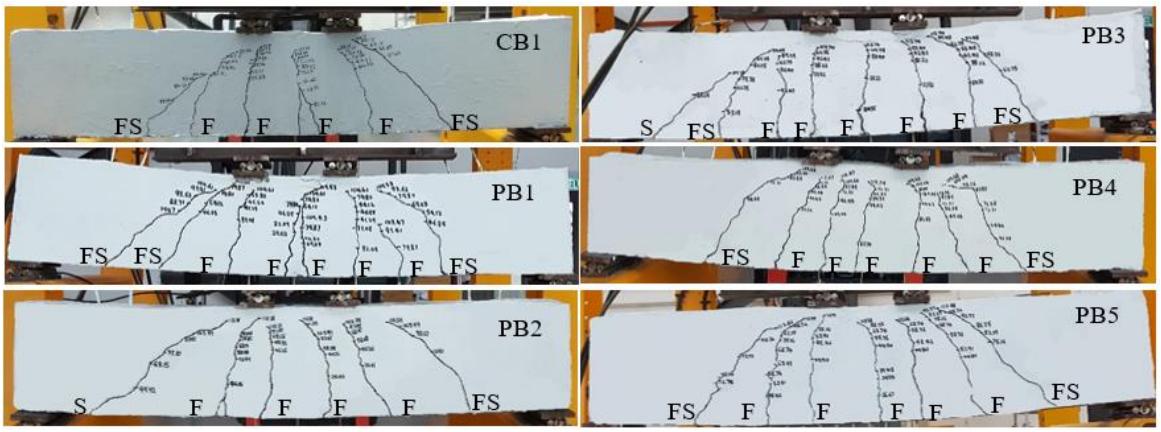

Figure 5. Crack pattern.

The failure mode implied critical damage to the specimen. It was determined based on the crack pattern and the severity of the cracks. The severity of the cracks was determined based on the crack length, the crack width, and the highest load achieved by the cracks [1]. All the specimens experienced diagonal tension failure (Figure 5 and Table 9).

Table 9. Type of failure mode [1].

	Flexural failure	Diagonal tension	Shear compression
Description	• The flexural cracks were dominant. • The flexural-shear crack may or may not be present. • No shear crack was noticed.	• The flexural-shear cracks were dominant. • Shear crack may or may not be present.	• The shear crack was dominant. • The shear crack may or may not reach the top reinforcement in the beam • The top beam may or may not be crushed.
Definition criteria	• The width of the flexural crack was the largest, and/or • The length of the flexural crack was the longest, and/or • The recorded load for the flexural crack was the highest	• The width of the flexural-shear crack was the largest, and/or • The length of the flexural-shear crack was the longest or at least comparable to the shear crack, and/or • The recorded load for the flexural-shear crack was the highest	• The width of the shear crack was the largest, and/or • The length of the shear crack was the longest, and/or • The recorded load for the shear crack was the highest

3.5. Test results.

Table 10 displays the specimen test results. The computation of these results is briefly described in Table 11 and Figure 6. The test specimens were then compared with the control specimen using performance ratios (Table 12). The beams with embedded polystyrene spheres were generally inferior to the solid beam. They had lower first crack, stiffness, and yield strength than the solid beam. The respective performance ratios in Table 12 were less than 1.0. This finding was in line with the observation by Mohamad et al. (2017) [13]. Their beams with HDPE plastic balls also had a lower first crack load than the solid beam.

Table 10. Test results.

Specimen	Elastic stage				Yield stage		Ultimate stage			
	P_{cr} (kN)	δ_{cr} (mm)	S_i (kN/mm)	S_s (kN/mm)	P_y (kN)	δ_y (mm)	P_u (kN)	δ_u (mm)	Δ	Failure mode
CB	31.0	0.97	32.0	18.8	107.4	6.30	118.4	30.0	4.76	DT
PB1	29.0	0.95	30.5	18.5	103.9	6.48	119.8	31.1	4.80	DT
PB2	28.7	0.96	29.9	18.0	102.7	6.57	118.3	31.6	4.81	DT
PB3	24.3	1.10	22.1	11.1	101.9	10.51	116.7	34.2	3.25	DT
PB4	25.7	1.11	23.2	11.8	102.9	9.92	117.0	34.0	3.42	DT
PB5	26.7	1.16	23.0	14.5	100.7	8.10	117.4	33.5	4.14	DT

P_{cr} = first crack load, δ_{cr} = first crack deflection, S_i = Initial stiffness, S_s = Secant stiffness ($0.75P_u$), P_y = yield load, δ_y = yield displacement, P_u = ultimate load, δ_u = ultimate displacement, Δ = ductility ratio

Table 11. Computation of the results.

Results	Description
First crack load, P_{cr}	The load when the first crack was noticed, as acquired from Figure 5.
First crack deflection, δ_{cr}	The specimen's deflection when the first crack was noticed. It was obtained from the load-displacement curve in Figure 4.
Initial stiffness (uncracked), S_i	The stiffness of the specimen before cracking (Figure 6(a)). It was calculated using the equation $S_i = \frac{P_{cr}}{\delta_{cr}}$.
Secant stiffness, S_s	The specimen's elastic stiffness. It was calculated as the gradient of the line passing through the point of $0.75P_u$ (Figure 6(b)).
Yield point (P_y, δ_y)	A point on the load-displacement curve where plastic deformation of the specimen was initiated. It was determined by using the method used by Ling et al. (2020) [31], as demonstrated in Figure 6(b).
Ultimate load, P_u	The load capacity of the specimen was the highest point of the load-displacement curve (Figure 4).
Ultimate deflection, δ_u	The deflection of the specimen when the load peaked (Figure 4).
Ductility, Δ	An index representing the ductile behaviour of the specimen, which was computed using the equation, $\Delta = \frac{\delta_u}{\delta_y}$.

Table 12. Performance of test specimens relative to the control specimen.

Specimen	Performance ratios					
	$\frac{P_{cr,i}}{P_{cr,c}}$	$\frac{S_{i,i}}{S_{i,c}}$	$\frac{S_{s,i}}{S_{s,c}}$	$\frac{P_{y,i}}{P_{y,c}}$	$\frac{P_{u,i}}{P_{u,c}}$	$\frac{\Delta_i}{\Delta_c}$
PB1	0.94	0.95	0.98	0.97	1.01	1.01
PB2	0.93	0.93	0.96	0.96	1.00	1.01
PB3	0.78	0.69	0.59	0.95	0.99	0.68
PB4	0.83	0.73	0.63	0.96	0.99	0.72
PB5	0.86	0.72	0.77	0.94	0.99	0.87

For test specimens: $P_{cr,i}$ = first crack load, $S_{i,i}$ = initial stiffness, $S_{s,i}$ = secant stiffness, $P_{y,i}$ = yield load, $P_{u,i}$ = ultimate load, Δ_i = ductility ratio. For control specimen: $P_{cr,c}$ = first crack load, $S_{i,c}$ = initial stiffness, $S_{s,c}$ = secant stiffness, $P_{y,c}$ = yield load, $P_{u,c}$ = ultimate load, Δ_c = ductility ratio

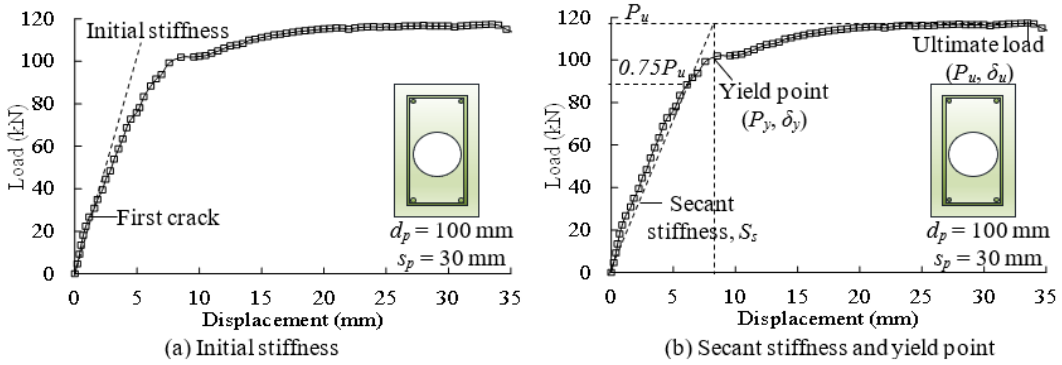

(a) Initial stiffness (b) Secant stiffness and yield point

Figure 6. Computation of specimen's properties (PB5).

3.6. Effects of polystyrene spheres on beam's stiffness.

The initial stiffness and secant stiffness represent the behavior of the specimen before and after cracking, respectively. The initial stiffness was always greater than the secant stiffness (Table 10). This was regardless of the solid beam or the beams with embedded polystyrene spheres. Before cracking, steel reinforcement and concrete resisted the flexural stress together. The elastic moduli of the two materials contributed to the high initial stiffness. After cracking, the concrete gave way under the tensile stress. As a result, the reinforcements took on all of the stress. This slightly reduced the beam's stiffness. The polystyrene spheres reduced both the initial and secant stiffness of the beam. The performance ratios $S_{i,i}/S_{i,c}$ and $S_{s,i}/S_{s,c}$ of specimens PB1 to PB5 were all less than 1.0 (Table 12). The polystyrene spheres reduced the moment of inertia of the section. This had an effect on the beams' ability to withstand bending moments [32].

The beam's stiffness decreased as the polystyrene spheres' diameter increased. This can be seen in specimens PB1, PB2, and PB3. The surface stiffness decreased by 40% from 18.5 kN/mm to 11.1 kN/mm as the polystyrene spheres' diameter increased from 50 mm to 100 mm. As the diameter increased from 50 mm to 100 mm, the concrete replacement increased from 1.9% to 8.7% (Table 6). The moment of inertia decreased when more concrete was replaced. This affected the stiffness (i.e., resistance to bending deformation) of the beam [32]. The spacing between the polystyrene spheres also influenced the beam's stiffness. This was proven by specimens PB3, PB4, and PB5. As the spacing increased from 10 mm to 30 mm, the nominal stiffness increased by 30%, from 11.1 kN/mm to 14.5 kN/mm. The spacing between the polystyrene spheres formed a series of ribs in the beam. The ribs provided resistance to the beam's deformation under load. The larger the ribs around the polystyrene spheres, the higher the stiffness of the beam. This finding was in line with the studies by Izzat et al. (2014) [33] and Lim (2020) [34]. Their specimens performed better with larger ribs between the lightweight materials.

3.7. Effects of polystyrene spheres on beam's strength.

There were three types of strength obtained. The uncracked strength was the beam strength before the first crack. The yield strength marked the beginning of the plastic deformation of the beam. The ultimate strength represented the load capacity of the beam.

As the diameter of the polystyrene sphere increased from 50 mm to 100 mm: (Table 10)

- the uncracked strength decreased by 16.2%, from 29 kN to 24.3 kN.
- the yield strength decreased by 1.9%, falling from 103.9 kN to 101.9 kN, and
- the ultimate strength was reduced by 2.6%, dropping from 119.8 kN to 116.7 kN.

When the spacing between polystyrene spheres increased from 10 mm to 30 mm: (Table 10)

- the uncracked strength increased by 9.8% from 24.3 kN to 26.7 kN.
- the yield strength was influenced marginally within a range of +/-1.1%, and
- the ultimate strength increased by 0.6%, rising from 116.7 kN to 117.4 kN.

Based on these observations, the uncracked strength was more severely affected by the polystyrene spheres than the yield strength or the ultimate strength. The spheres substituted for the concrete and altered the geometrical properties of the beam's section. This impeded the distribution of stress in the beam, where higher stress was concentrated near the beam's soffit. Subsequently, the larger concrete strain caused the beam to quickly crack. To delay the first crack, polystyrene spheres may be placed further away from the soffit [22].

3.8. Effects of polystyrene spheres on beam's ductility.

Ductility reflects the ability of a beam to deform significantly under excessive load. It provides warnings before the beam failed. The size of the polystyrene influenced the ductility of the test specimens. This can be observed from specimens PB1, PB2, and PB3 (Table 10). When the polystyrene sphere's diameter was 75 mm or less, the ductility was comparable to that of the solid beam. The ductility of the beam was 32% lower than the solid beam when 100 mm polystyrene spheres were used. A similar observation was reported by Lim et al. (2021) [21]. Their beams with embedded polystyrene blocks also had a lower ductility than the solid beam.

The ductility was also affected by the spacing between the polystyrene spheres. This was observed in specimens PB3, PB4, and PB5. The ductility increased 27% from 3.25 to 4.14 when the spacing increased from 10 mm to 30 mm.

4. Feasibility Evaluation

The feasibility of the beam with polystyrene spheres was evaluated in various aspects. This included weight reduction, material efficiency, load capacity, serviceability, ductility, and failure modes.

The evaluation criteria are outlined as follows:

a. C1: The polystyrene spheres should replace a large amount of concrete so that the reduction in the specimen's weight is meaningful. The volume replacement ratio, R_v, (Table 6) was preferably at least the mean value of the test specimens, which was 5.94%.

b. C2: The beam with polystyrene spheres should be more efficient than the solid beam. The strength per unit of concrete of the test specimen should be greater than that of the control specimen. Thus, the effective strength-volume ratio, R_e, should theoretically be at least 1.0 [20]. Since all the test specimens had R_e greater than 1.0, the mean value of all specimens was benchmarked.

$$R_e = \frac{E_b}{E_s} \geq 1.058 \quad (8)$$

where E_b = strength per unit concrete of the beam with polystyrene spheres, kN/m^3; E_s = strength per unit concrete of the solid beam, kN/m^3.

The strengths per unit of concrete (i.e. E_b and E_s) were determined by dividing the load capacity by the total concrete volume of the beam.

c. C3: The beam with polystyrene spheres should have a larger load capacity than the solid beam. Thus, the strength ratio, R_s, should be at least 1.0.

$$R_s = \frac{P_{u,i}}{P_{u,s}} \geq 1.0 \quad (9)$$

where $P_{u,i}$ = ultimate strength of the beam with polystyrene spheres, kN; $P_{u,s}$ = ultimate strength of the solid beam, kN.

d. C4: The service load of the beam with polystyrene spheres should not be too low compared with its load capacity. Thus, the serviceability ratio, R_{sv}, should be at least 0.75 [35, 36].

$$R_{sv} = \frac{P_y}{P_u} \geq 0.75 \quad (10)$$

where P_y = yield strength of the beam with polystyrene spheres, kN; P_u = ultimate strength of the beam with polystyrene spheres, kN.

e. C5: The beam with polystyrene spheres should have adequate ductility for survival purposes. The ductility ratio, Δ, should be at least 4.0 for the application in the low to moderate seismic regions [20, 35, 37, 38].

$$\Delta = \frac{\delta_u}{\delta_y} \geq 4.0 \quad (11)$$

where δ_u = ultimate displacement of the beam with polystyrene spheres, mm; δ_y = yield displacement of the beam with polystyrene spheres, mm.

f. C6: The failure mode of the beam with polystyrene spheres should be similar to that of a solid beam. Substituting the concrete with polystyrene spheres reduced the beam's shear strength. For a typical flexural load test, the specimen was preferred without the shear crack.

Each specimen was evaluated based on criteria C1 to C6 (Table 13). None of the specimens fulfilled all the criteria. Thus, the specimen that met the most criteria was identified. Specimen PB5 satisfied all the criteria except C3. Its strength ratio, R_s, of 0.99 was slightly below the requirement of 1.0. This was considered acceptable. Thus, specimen PB5 could be used for structural application. Its specifications included (a) the size of polystyrene spheres equalled 0.57 times the beam's width, and (b) the spacing between polystyrene spheres was 1.2 times the concrete cover.

Table 13. Feasibility evaluation of the test specimen.

Criteria [1]	**C1**		**C2**		**C3**	**C4**	**C5**	**C6**		
	R_v	V_b (mm^3)	E_b (N/mm^3)	R_e	R_s	R_{sv}	Δ	n_s	**Score** [2]	**Remark** [3]
Ref.	Table 6			Eq. 8	Eq. 9	Eq. 10	Eq. 11	Figure 5		
Req.	≥0.0594			≥1.058	≥1.0	≥0.75	≥4.0	<1		
PB1	0.019	82,363,754	0.001455	1.03	1.01	0.87	4.80	0	4/6	NA
PB2	0.047	80,023,922	0.001478	1.05	1.00	0.87	4.81	1	3/6	NA
PB3	0.087	76,669,617	0.001522	1.08	0.99	0.87	3.25	1	3/6	NA
PB4	0.075	77,716,815	0.001505	1.07	0.99	0.88	3.42	0	4/6	NA
PB5	0.069	78,240,413	0.001501	1.06	0.99	0.86	4.14	0	5/6	A
Mean	0.0594			1.058						

[1] R_v = volume replacement ratio, V_b = concrete volume of beam ($V_b = V_s - V_p$), P_u and P_y refer to Table 10, E_b = strength per unit concrete of beam, R_e = effective strength ratio, R_s = strength ratio, R_{sv} = serviceability ratio, Δ = ductility ratio, n_s = nos. of shear crack found on beam surface.
[2] Nos. of evaluation criteria met out of six
[3] A – Applicable, NA – Not applicable

It is worth mentioning that this study ignored the weight and strength of polystyrene spheres. The concrete region occupied by the polystyrene spheres was assumed to be void, which carried no stress. The volume of polystyrene spheres in the beam was deemed equal to the weight reduction. This was conditional on the homogeneity of the concrete throughout the beam. As an exploratory study, only one specimen was tested for each design. Out of the limited data, it seemed the beam with polystyrene spheres was more efficient than the solid beam. There have also been studies that show a discernible loss of strength in hollow beam sections [1, 30]. For some reason, the two types of beams were similar, but the outcome varied. Further studies may be required to find out the reasons.

6. Conclusions

This study investigated the behavior of beams with embedded polystyrene spheres under loads. This technique can improve the material's efficiency. The beam's strength per unit of concrete increased by 8% when polystyrene spheres replaced 8.7% of the concrete volume. Polystyrene spheres marginally affected the beam's strength. The strength dropped by 2.6% as the diameter of the polystyrene spheres increased from 50 mm to 100 mm. The load capacity increased by

0.6% as the spacing increased from 10 mm to 30 mm. The diameter and spacing of the polystyrene spheres did not appear to have a significant effect on the beam's strength. Compared with the solid beam, the beams with polystyrene spheres generally had lower uncracked strength, stiffness, and ductility. PB5 outperformed the other specimens. It met almost all of the evaluation criteria. Nevertheless, there is no explicit guide for evaluating a beam's feasibility. The evaluation was mainly based on the preferred states of the specimens. Specimen PB5 can be expressed in generic specifications: the size of the polystyrene spheres equals 0.57 times the beam's width, and the spacing between polystyrene spheres is 1.2 times the concrete cover. This might be a reference for future studies with the conditions that the polystyrene spheres are placed at the centroid of the cross-section and the beam's width is smaller than its height. One may need to verify whether or not those specifications apply to beams of other sizes and aspect ratios.

Acknowledgments

This research work was supported by the Research Grants of University of Technology Sarawak UCTS/ RESEARCH/2/2018/02.

Competing Interest

The authors declare no conflict of interest.

References

[1] Ling, J.H.; Ngu, J.T.S.; Lim, Y.T.; Leong, W.K.; Sia, H.T. (2022). Experimental study of RC hollow beams with embedded PVC pipes. *Journal of Advanced Civil and Environmental Engineering, 5,* 11–23. https://doi.org/10.30659/jacee.5.1.11-23.

[2] Ali, S.; Kumar, M. (2017). Analytical study of conventional slab and bubble deck slab under various support and loading conditions using Ansys Workbench 14.0. *International Research Journal of Engineering and Technology, 4*, 1467–1472.

[3] Ling, J.H.; Chan, L.L.; Leong, W.K.; Sia, H.T. (2020). The development of finite element model to investigate the structural performance of reinforced concrete hollow beams. *Journal of the Civil Engineering Forum, 6*, 171–182. https://doi.org/10.22146/jcef.53301.

[4] Mohd Noh, H.; Azwani Mohamad, N.L.I.; Bangau, R. (2020). Performance of hollow reinforced concrete beam in structural member. *Journal of Mechanical Engineering, 17,* 1–11. https://doi.org/10.24191/jmeche.v17i2.15296.

[5] Joy, J.; Rajeev, R. (2014). Effect of reinforced concrete beam with hollow neutral axis. *International Journal for Scientific Research & Development, 2,* 341–348.

[6] Parthiban, N.; Neelamegam, M. (2017). Flexural behavior of reinforced concrete beam with hollow core in shear section. *International Research Journal of Engineering and Technology, 4,* 2263–2274.

[7] Al-Gasham, T.S.S. (2015). Reinforced concrete moderate deep beams with embedded PVC pipes. *Wasit Journal of Engineering Science, Volume 3,* 19–28. http://doi.org/10.31185/ejuow.Vol3.Iss1.32.

[8] Idris, N.A.; Mohd Noh, H. Azwani Mohamad, N.L.I.; Bangau, R. (2020). Reinforced Concrete by Using the Rectangular Shape of Voided Beam. *Journal of Mechanical Engineering 9,* 179-190.

[9] Balaji, G.; Vetturayasudharsanan, R. (2020). Experimental investigation on flexural behaviour of RC hollow beams. *Materialstoday: Proceeding, 21,* 351–356. https://doi.org/10.1016/j.matpr.2019.05.461.

[10] Hassan, N.Z.; Ismael, H.M.; Salman, A.M. (2018). Study behavior of hollow reinforced concrete beams. *International Journal of Current Engineering and Technology, 8,* 1640–1651. https://doi.org/10.14741/ijcet/v.8.6.19.

[11] Al-Badkubi, M.R.K.M. (2019). Finite element study on ultimate shear capacity of voided reinforced concrete beams. 2nd International Conference on Engineering Technology and their Applications, Alnajaf-Iraq. https://doi.org/10.1109/IICETA47481.2019.9012987.

[12] Ajeel, A.E.; Qaseem, T.A.; Rasheed, S.R. (2018). Structural behavior of voided reinforced concrete beams under combined moments. *Civil and Environmental Research, 10*, 17–24.

[13] Mohamad, N.; Goh, W.I.; Samad, A.A.A.; Lockman, A.; Alalwani, A. (2017). Structural behaviour of beam with HDPE plastic balls subjected to flexural load. *Materials Science Forum, 889*, 270–274. https://doi.org/10.4028/www.scientific.net/MSF.889.270.

[14] Patel, R.R. (2018). Flexural behavior and strength of doubly-reinforced concrete beams with hollow plastic spheres. Master thesis, Old Dominion University, Virginia.

[15] Al-Badkubi, M.R.K.M. (2018). Finite element study on flexural behavior of voided concrete beams. *International Journal of Civil Engineering and Technology, 9*, 123–138.

[16] Mathew, I., Varghese, S.M. (2016). Experimental study on partial replacement of concrete in and below neutral axis of beam. *International Journal of Innovative Research & Technology, 3,* 188–192.

[17] Sariman, S.; Nurdin, A.R. (2018). Flexural behavior of T shaped reinforced concrete hollow beam with plastic bottle waste. *International Journal of Civil Engineering and Technology*, *9*, 534–543.

[18] Sivaneshan, P.; Harishankar, S. (2017) Experimental study on voided reinforced concrete beams with polythene balls, *IOP Conf. Series: Earth and Environmental Science, 80,* 1–8. https://doi.org/10.1088/1755-1315/80/1/012031.

[19] Jose, B.T.; Sasi, D. (2018). Comparative study on partial replacement of concrete below neutral axis of beam using seeding trays and polythene balls. *International Journal of Innovative Science, Engineering & Technology*, *5*, 172–177.

[20] Lau, J.W., Ling, J.H., Lim, Y.T. (2020). Feasibility study of reinforced concrete beam with embedded polystyrene spheres under incremental flexural load. *Borneo Journal of Social Science & Technology, 2,* 11–26. http://doi.org/10.3570/bjost.2020.2.2-04.

[21] Lim, Y.T.; Ling, J.H.; Lau, J.W.; Yik, A.Y.M. (2021). Experimental study on the flexural behavior of reinforced polystyrene blocks in concrete beams. *Journal of the Civil Engineering Forum, 7,* 197–208. https://doi.org/10.22146/jcef.62346.

[22] Lim, Y.T., Ling, J.H., Lau, J.W., Danson, T.T.L. (2021). Performance of reinforced concrete beam with polystyrene blocks at various regions. *Journal of Science and Applied Engineering, 3,* 62–71. https://doi.org/10.31328/jsae.v3i2.1655.

[23] Tan, D.T.L., Ling, J.H. (2020). Flexural behaviour of reinforced concrete beam embedded with different alignment of polystyrene. *Borneo Journal of Sciences and Technology, 2,* 13–18. https://doi.org/10.35370/bjost.2020.2.1-04.

[24] Manikandan, S.; Dharmar, S.; Robertravi, S. (2015). Experimental study on flexural behaviour of reinforced concrete hollow core sandwich beam. *International Journal of Advance Research in Science and Engineering, 4,* 937–946.

[25] Jaini, Z.M.; Koh, H.B.; Mokhatar, S.N.; Mat, I.; Hazmi, H.; Hashim, N.H. (2016). Structural behaviour of short-span reinforced concrete beams with foamed concrete infill. *ARPN Journal of Engineering and Applied Sciences, 11,* 9820–9824.

[26] Kumbhar, U.N., Jadhav, H.S. (2018). Flexural behaviour of reinforced concrete hollow beam with polypropylene plastic sheet infill. *International Research Journal of Engineering and Technology, 5,* 1517.

[27] Ragavi, L. (2017). Behaviour of reinforced concrete hollow beams under monotonic loading. *World Journal of Technology, Engineering and Research, 2,* 127–136.

[28] Alshimmeri, A.J.H.; Al-Maliki, H.N.G. (2014). Structural behavior of reinforced concrete hollow beams under partial uniformly distributed load. *Journal of Engineering, 20*, 130–145.
[29] Casturi H.; Hanumantha Rao, C. (2020). Analysis of composite hollow RC beam strengthened with mild steel sections. *Materials Today: Proceedings*, *33*, 687–694, https://doi.org/10.1016/j.matpr.2020.05.813.
[30] Lim, Y.T., Ling, J.H. (2019). Incorporating lightweight materials in reinforced concrete beams and slabs - a review. *Borneo Journal of Sciences and Technology*, *1*, 16–26. https://doi.org/10.35370/bjost.2019.1.2-03.
[31] Ling, J. H., Tang, H. S., Leong, W. K., Sia, H. T. (2020). Behaviour of reinforced concrete beams with circular transverse openings under static loads, *Journal of Science and Applied Engineering*, *3*, 1–16, https://doi.org/10.31328/jsae.v3i1.1288.
[32] Bailey, C.; Bull, T.; Lawrence, A. (2013). The bending of beams and the second moment of area. *The Plymouth Student Scientist, 6,* 328–339.
[33] Izzat, A.F.; Farhan, J.A.; Allawi, N.M. (2014). Behaviour and strength of one way reinforced concrete slabs with cavities. International Conference for Engineering Science, University of Mustansiriyah, Baghdad.
[34] Lim Y.T. (2020). Performance of reinforced concrete beams with polystyrene as partial concrete replacement material under flexural loads. Master thesis, University College of Technology Sarawak, Malaysia.
[35] Ling, J.H.; Abd. Rahman, A.B.; Ibrahim, I.S.; Abdul Hamid, Z. (2017). An experimental study of welded bar sleeve wall panel connection under tensile, shear, and flexural loads, *International Journal of Concrete Structures and Materials, 11*, 525–540. https://doi.org/10.1007/s40069-017-0202-y.
[36] Ling, J.H.; Abd. Rahman, A.B.; Ibrahim, I.S. (2022). Deformation behavior of grouted sleeve wall connector under shear load in precast process of concrete wall. *Indonesian Journal of Computing, Engineering, and Design, 4,* 1–14. https://doi.org/10.35806/ijoced.v4i2.263.
[37] Soudki, K.A. (1994). Behaviour of horizontal connections for precast concrete load-bearing shear wall panels subjected to reversed cyclic deformations. PhD thesis, University of Manitoba, Canada.
[38] Ling, J.H.; Lim, J.H.; Abd. Rahman, A.B. (2021). Behaviour of precast concrete beam-to-column connection with shs hidden corbel subjected to monotonic load. *Journal of the Civil Engineering Forum, 7*, 223–238 https://doi.org/10.22146/jcef.62930.